

# Long-period eclipsing binaries: towards the true mass-luminosity relation.

## I. the test sample, observations and data analysis

Alexei Yu. Kniazev<sup>1,2,3</sup>, Oleg Yu. Malkov<sup>4</sup>, Ivan Yu. Katkov<sup>3,5,6</sup> and Leonid N. Berdnikov<sup>3</sup>

<sup>1</sup> South African Astronomical Observatory, P.O. Box 9, Observatory, Cape Town, 7935, South Africa; [aknizev@sao.ac.za](mailto:aknizev@sao.ac.za)

<sup>2</sup> Southern African Large Telescope, P.O. Box 9, Observatory, Cape Town, 7935, South Africa

<sup>3</sup> Sternberg Astronomical Institute, Lomonosov Moscow State University, Moscow, 119992, Russia

<sup>4</sup> Institute of Astronomy of RAS, Moscow 119017, Russia

<sup>5</sup> New York University Abu Dhabi, PO Box 129188, Abu Dhabi, UAE

<sup>6</sup> Center for Astro, Particle, and Planetary Physics, NYU Abu Dhabi, PO Box 129188, Abu Dhabi, UAE

Received 2020 January 27; accepted 2020 March 24

**Abstract** The mass-luminosity relation is a fundamental law of astrophysics. We have suggested that the currently used mass-luminosity relation is not correct for the  $M/M_{\odot} > 2.7$  range of mass since it was created utilizing double-lined eclipsing binaries, where the components are synchronized and consequently change each other's evolutionary path. To exclude this effect, we have started a project to study long-period massive eclipsing binaries in order to construct radial velocity curves and determine masses for the components. We outline our project and present the selected test sample together with the first HRS/SALT spectral observations and the software package, FITTING BINARY STARS (FBS), that we developed for the analysis of our spectral data. As the first result, we present the radial velocity curves and best-fit orbital elements for the two components of the FP Car binary system from our test sample.

**Key words:** stars: luminosity function, mass function — stars: binaries: spectroscopic

## 1 INTRODUCTION

The mass of a star is, to a first approximation, the most important parameter in determining its evolution. However, the mass cannot be dynamically determined for a single star, so indirect methods have been developed for estimating stellar masses. The most widely employed of them is to estimate the mass from observations of the distribution of another parameter for a stellar ensemble under study (field stars, cluster stars). Stellar luminosity is the most commonly considered parameter, and the subsequent transition to masses of stars is made by applying the so-called mass-luminosity relation (MLR).

Independent determination of the mass of a star and its luminosity is only possible for components of binary systems of certain types.

One suitable type of binary system is a visual binary star with known orbital parameters and trigonometric parallax. Such stars are usually wide pairs, whose components do not interact with each other and are evolutionarily similar to single stars. In addition, usually they are in the near-

by solar neighborhood and, therefore, are mostly low-mass stars. The problem of determining the masses of visual binaries was discussed, for example, in [Docobo et al. \(2016\)](#), [Malkov et al. \(2012\)](#) and [Fernandes et al. \(1998\)](#). The construction of the MLR for low-mass stars based on observational data is discussed in [Henry \(2004\)](#), [Delfosse et al. \(2000\)](#), [Henry et al. \(1999\)](#) and [Malkov et al. \(1997\)](#).

Another major source of independently defined stellar masses is detached eclipsing binary stars with components on the main sequence, where the spectral lines of both components are observed (hereafter double-lined eclipsing binaries, DLEBs). These stars are usually relatively massive ( $M/M_{\odot} > 1.5$ ) and their parameters are utilized to construct the stellar MLR for intermediate and large masses. The exact parameters of DLEB stars and the MLR based on them can be found, for example, in [Torres et al. \(2010\)](#), [Kovaleva \(2001\)](#), [Gorda & Svechnikov \(1998\)](#), [Andersen \(1991\)](#) and [Popper \(1980\)](#).

When these two MLRs (based on visual binaries and on the DLEB stars with components on the main sequence) are jointly analyzed and used (in particular, in order to

compare the theoretical MLRs with empirical data), it is generally assumed, by default, that the components of the detached close binaries and the wide binaries evolve in a similar way. It should be noted, however, that DLEBs are close pairs whose components’ rotation is synchronized by tidal interaction, and, due to rotational deceleration, they evolve differently than “isolated” (i.e., single or wide binary systems) stars.

When comparing the radii of DLEBs and single stars (Malkov 2003), a noticeable difference between the observed parameters of B0V-G0V components for DLEBs and for single stars of similar spectral classes was found. This difference was confirmed by analysis of independent studies published by other authors. This difference also explains the disagreement between the published scales of bolometric corrections. Larger radii and higher temperatures of A-F components of DLEB stars can be explained by the synchronization and associated slowing down of rotation of such components in close systems. Another possible reason is the effect of observational selection: due to the non-sphericity of rotating stars, the parameters determined from the observations depend on the relative orientations of their rotation axes. Isolated stars are oriented randomly, while components of eclipsing binaries are usually observed from near the equatorial plane. Systematically smaller observed radii of DLEB stars in spectral class B can be explained by the fact that stars with large radii do not occur with companions on the main sequence: most of them have already filled their Roche lobe (which stopped their further growth) and have become semi-detached systems (which excluded them from the discussed statistics). Then, in Malkov (2007), data for the fundamental parameters of the components of a few currently known long-period DLEBs were collected. These stars presumably have not undergone synchronization of rotation with orbital period and therefore spin rapidly, and evolve similarly to single stars.

The theory of synchronization (and circularization) in close binary systems developed by Zahn (1975, 1977) is based on the mechanism of energy dissipation via dynamic tides in non-adiabatic surface layers of the component stars. Another theory was put forth by Tassoul (1987, 1988), and is based on tidal dissipation of the kinetic energy of large-scale meridional flows. In their critical reviews, Khaliullin & Khaliullina (2007, 2010) point out that both the circularization and synchronization timescales implied by these mechanisms differ by almost three orders of magnitude, and, based on an analysis of the observed rates of apsidal motion, show that the observed synchronization times agree with Zahn’s theory but are inconsistent with the shorter timescale proposed by Tassoul.

The synchronization time depends primarily on the stellar mass and binary separation. So, for example, according to Tassoul (1987), the synchronization time for orbital periods up to about 25 days is smaller than one-tenth of the main sequence lifetime of a  $3 M_{\odot}$  star.

The theories of synchronization mentioned above have been developed for early-type, massive stars with radiative envelopes (i.e., for stars with  $M/M_{\odot} > 1.5$ ). In the current work, to construct the MLR for “isolated” stars, we study DLEB stars in the range  $M/M_{\odot} > 2.7$ , as the masses of components for other types of binary stars (visual binaries, resolved spectroscopic binaries) rarely exceed this limit (stars in the range  $1.5 < M/M_{\odot} < 2.7$  will be considered later). According to the shorter timescale theory of Tassoul, the synchronization time becomes comparable to the main sequence lifetime of a  $2.7 M_{\odot}$  star for orbital periods of the order of 50–70 d (the longer timescale theory of Zahn predicts even shorter periods).

Currently, there is no way to properly estimate the degree to which the effect on the initial mass function (IMF) may be important for  $M > 2.7 M_{\odot}$ , as available observational data for that mass range are too poor to draw definite conclusions. For that reason, we have started a pilot project to study long-period massive eclipsing binaries to construct radial velocity curves and determine the masses of their components. Using published photometric data or light-curve solutions, we expect to obtain luminosities for the individual components. With accurate luminosity determinations, we plan to compare their location on the mass-luminosity diagram with the “standard” MLR. As a result of this pilot study, we plan to confirm that rapid and slow rotators satisfy different MLRs, which should be utilized for different purposes. Then the feasibility of a larger project, the construction of a reliable “fast rotators” MLR, will be considered. The data we obtain will also be utilized to establish mass-radius and mass-temperature relations.

## 2 THE TEST SAMPLE, OBSERVATIONS AND DATA REDUCTION

To compile the test sample for our pilot project, we referenced the Catalog of Eclipsing Variables (hereafter CEV; Malkov et al. 2007; Avvakumova et al. 2013; Avvakumova & Malkov 2014) from which we have carefully selected 11 massive long-period (i.e., presumably non-synchronized) detached main-sequence eclipsing systems that are presented in Table 1. The selected systems should have components with similar luminosities (i.e., can be observed as SB2 systems – spectroscopic binaries, where spectral lines from both components are visible) and guarantee an accurate determination of stellar parameters (in particular masses to 3%) of early-type stars composing them. We planned to obtain a minimum of five spectra for

**Table 1** The Test Sample

#	Name	RA (2000.0)	DEC (2000.0)	mag	$e$	Period
(1)	(2)	(3)	(4)	(5)	(6)	(7)
01	V883 Ara	16:51:45.10	-50:17:46.5	8.55	$\gg 0$	61.8740
02	KV CMa	06:50:52.67	-20:54:37.4	7.16	$\gg 0$	68.3842
03	V338 Car	11:13:52.31	-58:36:30.4	9.30	$= 0$	74.6429
04	V884 Mon	07:05:11.84	-11:06:02.4	9.13	$= 0$	123.2100
05	V766 Sgr	17:51:57.00	-28:17:02.0	10.80	$= 0$	147.1050
06	FP Car	11:04:35.87	-62:34:22.2	9.70	$= 0$	176.0270
07	V1108 Sgr	19:12:43.63	-18:08:12.0	11.50	$\gg 0$	46.5816
08	PW Pup	07:49:06.00	-31:07:42.6	9.20	$= 0$	158.0000
09	Mu Sgr	18:13:45.81	-21:03:31.8	3.80	$\gg 0$	180.5500
10	AL Vel	08:31:11.28	-47:39:57.4	8.60	$= 0$	96.1070
11	NN Del	20:46:49.22	+07:33:10.4	8.39	$\gg 0$	99.2684

targets with circular orbits ( $e = 0$ ) and a minimum of 10 spectra for targets with non-circular orbits ( $e \gg 0$ ). This number of spectra should be enough to find a credible orbital solution and to complete the science objectives.

All observations were obtained with the High Resolution Spectrograph (HRS; Barnes et al. 2008; Bramall et al. 2010, 2012; Crause et al. 2014) at the Southern African Large Telescope (SALT; Buckley et al. 2006; O’Donoghue et al. 2006). The HRS was operated in medium resolution (MR) mode, which provides a spectral resolution  $R \sim 36\,500\text{--}39\,000$ ; it has an input fiber diameter of 2.23 arcsec for both object and sky. All our echelle data were obtained during 2017–2019 and cover the total spectral range  $\approx 3900\text{--}8900\text{ \AA}$ , where both blue and red CCDs were employed with  $1 \times 1$  binning. All science observations were supported by the HRS Calibration Plan, which includes a set of bias frames at the beginning of each observational night and a set of flat-fields and a spectrum of a ThAr lamp once per week. Since the HRS is a vacuum echelle spectrograph installed inside a temperature-controlled enclosure, such a set of calibrations is enough to yield an average external velocity accuracy of  $300\text{ m s}^{-1}$  (Kniazev et al. 2019). HRS data underwent a primary reduction with the SALT science pipeline (Crawford et al. 2010), which includes overscan correction, bias subtractions and gain correction. After that, echelle spectroscopic reduction was carried out using the HRS pipeline described in detail in Kniazev et al. (2016, 2019).

### 3 FITTING BINARY STARS: FULL PIXEL FITTING METHOD

To analyze fully reduced HRS spectra of binary systems and to determine stellar atmosphere parameters for each component, such as effective temperature  $T_{\text{eff}}$ , surface gravity  $\log g$ , metallicity  $[Z/H]$  as well as stellar rotation  $v \sin i$  and line-of-sight velocities  $V_j$ , we developed a dedicated PYTHON-based package, FITTING BINARY STARS (FBS) (Katkov et al. 2020, in preparation). The FBS pack-

age implements a full pixel fitting approach to simultaneous approximation of multiple epoch spectra of a binary system by combining two synthetic stellar models using  $\chi^2$  minimization. The FBS package developed on top of the non-linear minimization LMFIT package (Newville et al. 2016) provides a high-level interface to many optimization methods (e.g., Levenberg-Marquardt, Powell, downhill simplex Nelder-Mead method, differential evolution, etc.).

During the evaluation of  $\chi^2$ , the FBS proceeds by the following steps: First, the FBS interpolates two stellar templates from the grid of synthetic stellar spectra for given sets of stellar atmosphere parameters ( $T_{\text{eff}}, \log g, [Z/H]$ )<sub>1,2</sub>. The interpolation has to be fast to work with high-resolution stellar spectra containing tens to hundreds of thousands of pixels in the spectral range under analysis. Therefore, we propose an algorithm where the FBS precalculates the Delaunay triangulation in three dimensions of stellar model parameters ( $T_{\text{eff}}, \log g, [Z/H]$ ) using nodes of the synthetic grid. Interpolating the FBS finds the simplex containing the given point, then averages the spectra from the simplex vertices with weights inversely proportional to the squared distance to the vertex. Such an algorithm is very fast and might work on regular as well as irregular model grids with missing nodes. Then, the model templates are broadened by individual stellar rotation  $v \sin i_{1,2}$  and shifted for the line-of-sight velocities  $V_1^j, V_2^j$  at the epoch of the  $j$ -th spectrum. The last two steps are to sum templates with weights  $w_{1,2}$  and multiply the spectrum by the extinction curve appropriate to the assumed  $E(B - V)$  or to multiply the final spectrum by a polynomial continuum to match the difference between the observed and synthetic spectra. In such an approach, the  $\chi^2$  value can be written as follows

$$\chi^2 = \sum_j \chi_j^2 = \sum_j \sum_{\lambda} \left( \frac{F_{\lambda}^j - M_{\lambda}^j}{\delta F_{\lambda}^j} \right)^2, \quad (1)$$

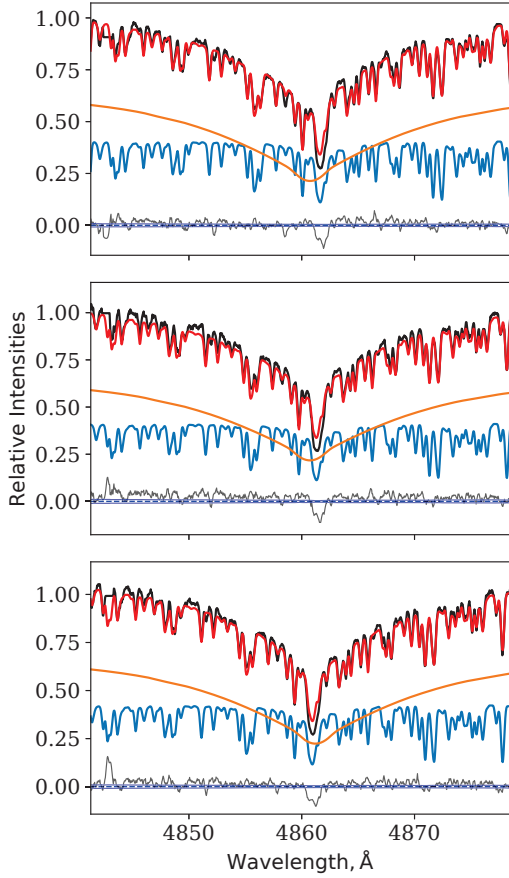


**Fig. 1** Example of the processing of three observed spectra of FP Car (three epochs) with the FBS software. Each panel displays part of the observed spectrum in the region of the  $H\beta$  line in black. The result of modeling is shown in red. The two components are signified in blue and orange, respectively. The difference between the observed and modeled spectra is depicted at the bottom of the panel in grey, together with errors that were propagated from the HRS data reduction (continuous dark blue lines).

$$M_{\lambda}^j = C_{\lambda} \sum_{k=1,2} w_k \cdot S(T_{\text{eff}k}, \log g_k, [Z/H]_k) * \mathcal{L}(V_k^j, v \sin i_k), \quad (2)$$

where  $F_{\lambda}^j$ ,  $\delta F_{\lambda}^j$ ,  $M_{\lambda}^j$  represent the observed spectrum at the  $j$ -th epoch, its uncertainties and the model, respectively;  $S$  is the stellar template interpolated from the grid of stellar models;  $\mathcal{L}$  is the convolution kernel to derive the broadening effect due to stellar rotation (Gray 1992) and to shift the templates by the line-of-sight velocity of each binary star component  $k$  at epoch  $j$ ; “\*” denotes convolution;  $C_{\lambda}$  is a polynomial multiplicative continuum or extinction curve for the given  $E(B - V)$ . The approach produces the following parameters:  $T_{\text{eff}}$ ,  $\log g$ ,  $[Z/H]$ ,  $v \sin i$  for both components of the binary star,  $n$  pairs of line-of-sight radial velocities  $V_1^j$ ,  $V_2^j$  for  $n$  spectra observed at different epochs and  $E(B - V)$  for the system.

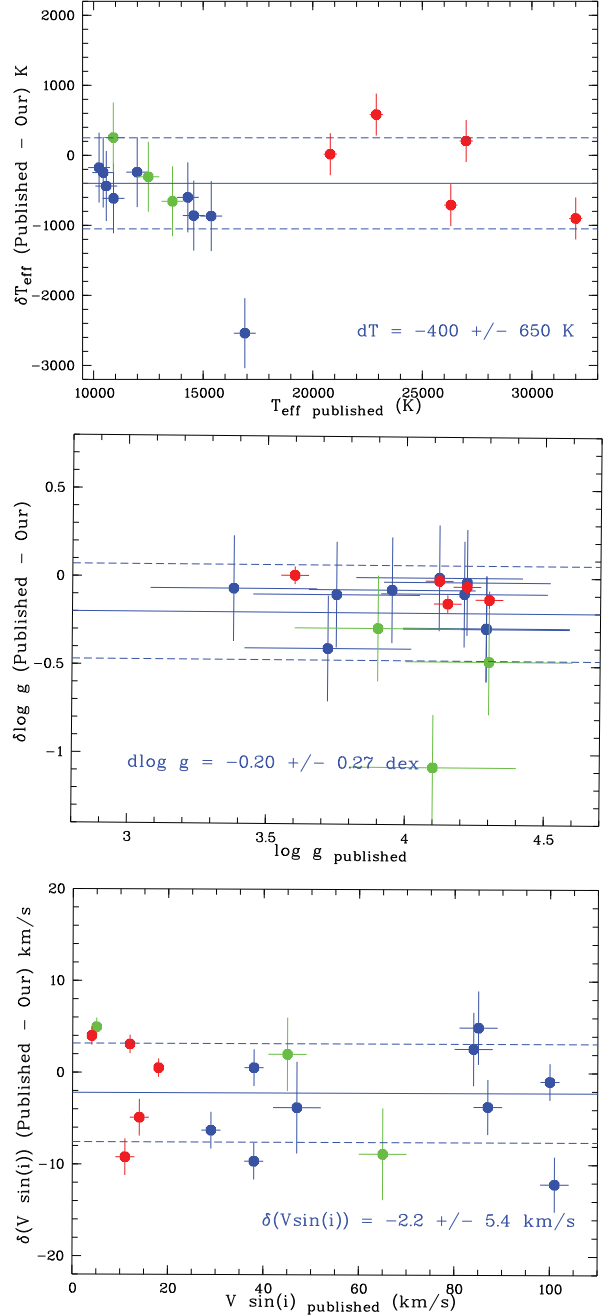


**Fig. 2** A comparison of the calculated  $T_{\text{eff}}$ ,  $\log g$  and  $v \sin i$ , from top to bottom respectively, with previously published results for the sample of early and late B-type stars.

Hereafter, we usually employ Coelho (2014) stellar models (stars with  $T_{\text{eff}} = 3000 - 26000$  K), which match the HRS MR instrumental resolution (Kniazev et al. 2019) well. Also we adapted high-resolution TLUSTY models ( $T_{\text{eff}} = 15000 - 55000$  K; Lanz & Hubeny 2003, 2007) and PHOENIX models ( $T_{\text{eff}} = 3000 - 23000$  K; Husser et al. 2013), convolving them to match the HRS MR instrumental resolution.

Due to the extensive functionality of the LMFIT package, the FBS provides flexible control over model parameters, including upper/lower bounding, parameter fixing and making parameters connected. As an example, connecting stellar component metallicities ( $[Z/H]_1 \equiv [Z/H]_2$ ) might be a reasonable approximation for binary stars formed in the same gas cloud. An example demonstrating the FBS software is featured in Figure 1 for three spectra of the binary system FP Car from our test sample. The FBS package is a full pixel fitting approach and allows us to approximate the full spectral range of the given spectrum or one or several spectral intervals as well as to easily mask bad pixels and/or spectral regions. The FBS package also contains basic functionality to determine orbital parameters from the stellar rotation curves.

#### 4 CHECK-UP OF THE EXTERNAL ACCURACY

To check the external accuracy of our FBS software, we performed different tests. For one of them, we fitted 18 echelle spectra of early and late B-type stars with the FBS program, which were obtained with the Fibre-fed Extended Range Optical Spectrograph (FEROS; [Kaufer et al. 1996](#)) and were modeled and published ([Hempel & Holweger 2003](#); [Nieva & Przybilla 2012](#); [Bailey & Landstreet 2013](#)). For this fit, we implemented models from [Coelho \(2014\)](#) for the late B-stars and models from [Lanz & Hubeny \(2003, 2007\)](#) for the early B-stars. The comparison of our results for  $T_{\text{eff}}$ ,  $\log g$  and  $v \sin i$  with results published earlier is shown in Figure 2. Our  $T_{\text{eff}}$  is comparable to that previously found with root mean square (rms) of 650 K,  $\log g$  with rms of 0.27 dex and  $v \sin i$  with rms of  $5.4 \text{ km s}^{-1}$ , which are very close to cited errors that are depicted with horizontal bars. There are no obvious systematic issues visible in this figure.

#### 5 FIRST RESULTS: THE FP CAR SYSTEM

As a first result, we would like to present here some of our results from study of the binary system FP Car that belongs to our test sample (see Table 1). FP Car (HD 96214), as a variable star with period of  $\sim 176$  d, was discovered by [Cannon \(1926\)](#). The period of this system was measured more accurately by [Dvorak \(2004\)](#) considering data from the All Sky Automated Survey (ASAS) ([Pojmanski 1997](#)). The spectral type was estimated by [Houk & Cowley \(1975\)](#) as B5/7(V). Approximate masses  $M_1 = 15.61 M_{\odot}$  and  $M_2 = 7.49 M_{\odot}$  for both components were calculated by [Brancewicz & Dworak \(1980\)](#) by implementing their iterative method for computation of geometric and physical parameters for components of eclipsing binary stars.

Our spectral observations of FP Car were acquired during 2017–2019 with HRS at SALT (see Sect. 2). Ten

spectra were obtained in total covering all phases of the binary’s orbit. After the standard HRS reduction, additionally, each HRS spectrum of FP Car was corrected for bad columns and pixels and was also corrected for the spectral sensitivity curve obtained closest to the date of the observation. Spectrophotometric standards for HRS were observed once a week as a part of the HRS Calibration Plan. Figure 3 presents one of a fully processed spectrum of FP Car, which was used in further analysis. The spectrum consists of 70 echelle orders from both the blue and red arms of HRS merged together and corrected for sensitivity. Unfortunately, SALT is a telescope where the unfilled entrance pupil of the telescope moves during the observation and for that reason, absolute flux calibration is not feasible with SALT. At the same time, since all optical elements are always the same, and relative flux calibration can be used for SALT data.

All HRS observations of the FP Car system were used simultaneously for the calculation of radial velocity curves employing the FBS package. Determination of orbital parameters from the stellar rotation curves was also done with the FBS package as is plotted in Figure 5 and presented in Table 2. The ascertained period is  $P = 176.032 \pm 0.010$  d which is in agreement within uncertainties with photometric period presented in Table 1. Our spectral data indicate that the system has a circular orbit ( $e = 0$ ) and this parameter was fixed for the last iteration. Our identified amplitudes of velocities have small errors of 0.7% for component B (blue) and 3.2% for component A (orange), which is totally in agreement with the fit shown in Figure 1, where the spectrum of component B exhibits many narrow lines and the spectrum of component A only manifests wide Balmer and helium lines with  $v \sin i \sim 100 \text{ km s}^{-1}$ . Finally, we can calculate masses of both components for the FP Car system as  $M_1 = (2.19 \pm 0.06) \sin^{-3}(i) M_{\odot}$  and  $M_2 = (1.42 \pm 0.06) \sin^{-3}(i) M_{\odot}$ , where  $i$  is the orbital inclination angle that can only be determined from modeling of photometric data. Unfortunately, there are no good photometric data for FP Car among all existing public surveys. The best available data are from the ASAS survey ([Pojmanski 1997](#)) as depicted in Figure 6. However, even these data have too few points outlining the positions and shapes of the narrow primary and secondary minima, and it is impossible to apply these data for any modeling. For that reason, we are actively accumulating photometric data for FP Car and other stars from our test sample utilizing the Las Cumbres Observatory (LCO) telescope network ([Brown et al. 2013](#)).

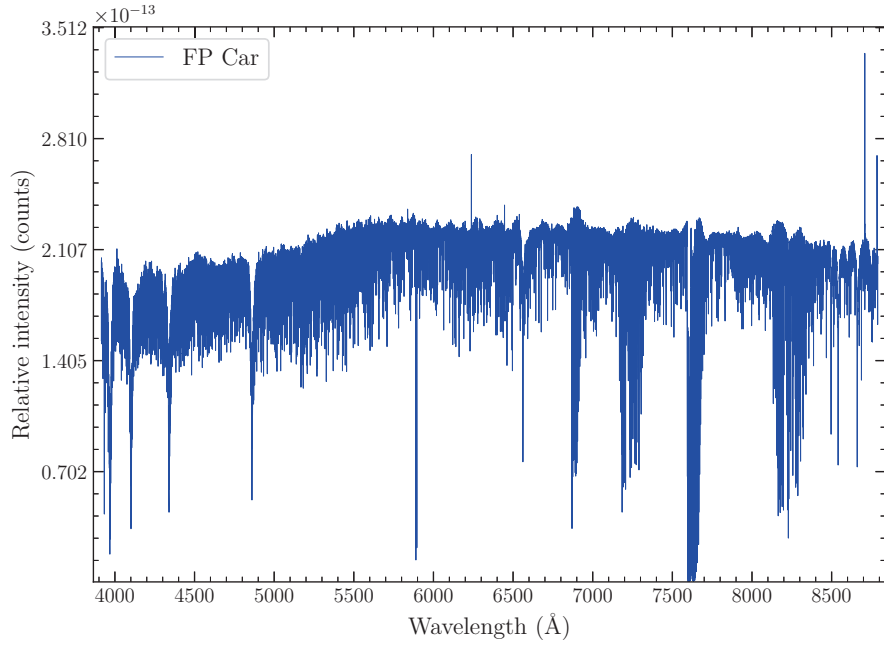


**Fig. 3** An example of a fully processed spectrum of FP Car. The spectrum consists of 70 echelle orders from both the blue and red arms merged together and corrected for the sensitivity curve.

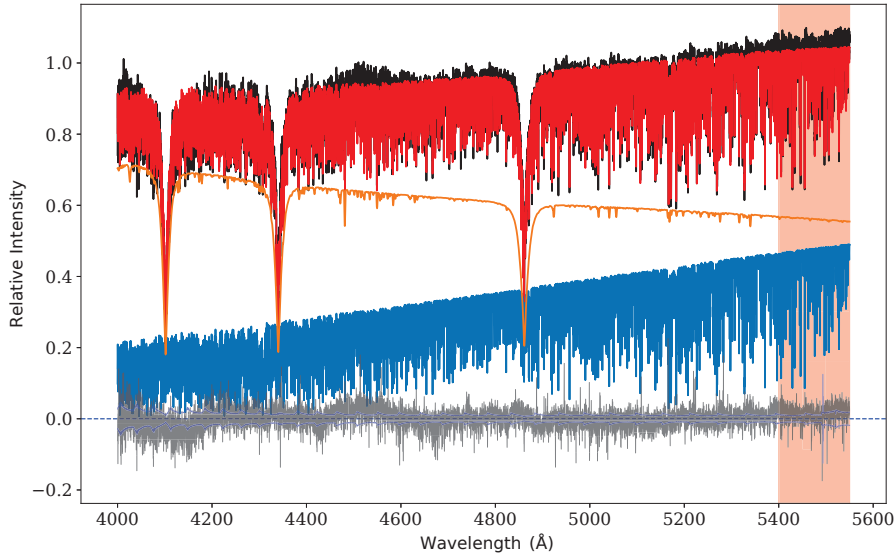


**Fig. 4** The results of the analysis of one spectrum of FP Car obtained with HRS. The panel depicts the result of the fit in the spectral region 4000–5300 Å. Designations are the same as in Fig. 1.

**Table 2** Best-fit Orbital Elements

Parameter	Value	%
Epoch at radial velocity maximum $T_0$ (d)	$2455094.47 \pm 0.15$	0.00
Orbital period $P$ (d)	$176.032 \pm 0.010$	0.00
Eccentricity $e$	0 (fixed)	0.00
Radial velocity semi-amplitude $K_1$ ( $\text{km s}^{-1}$ )	$22.92 \pm 0.73$	3.20
Radial velocity semi-amplitude $K_2$ ( $\text{km s}^{-1}$ )	$35.30 \pm 0.26$	0.72
Systemic heliocentric velocity $\gamma$ ( $\text{km s}^{-1}$ )	$-15.31 \pm 0.15$	0.96
rms residuals of Keplerian fit ( $\text{km s}^{-1}$ )	0.976	–

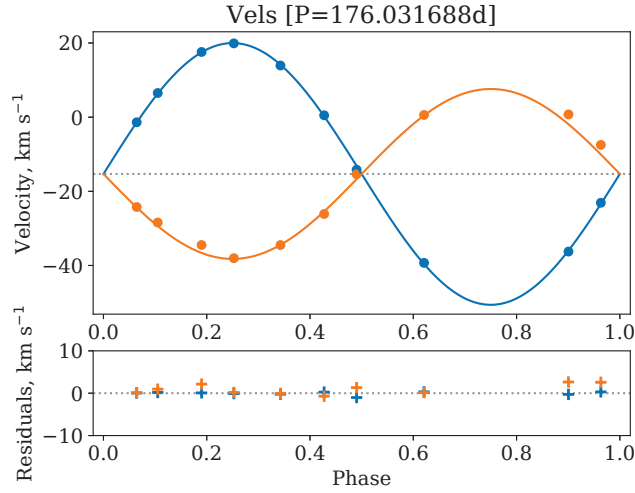


**Fig. 5** The calculated radial velocity curves for the FP Car binary system from our test sample.

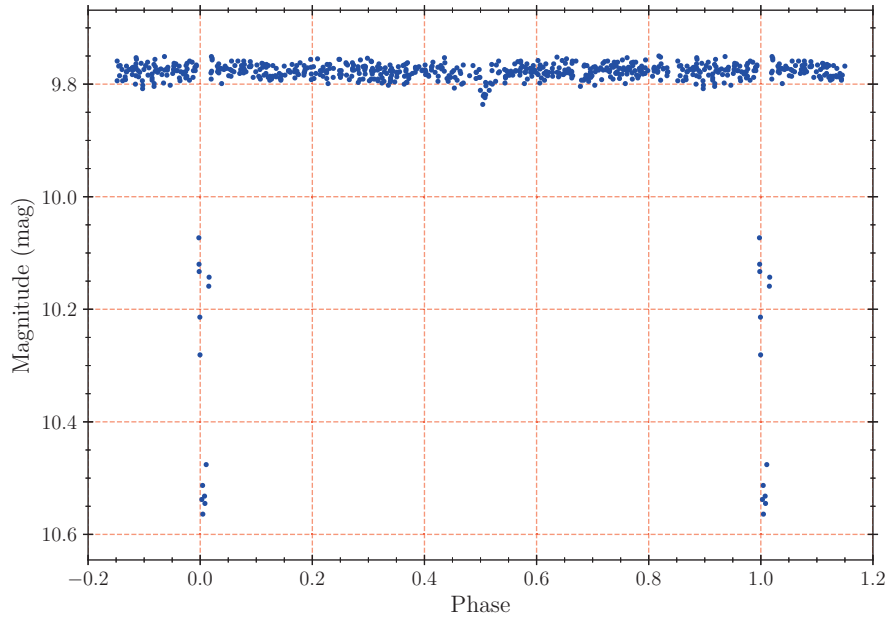


**Fig. 6** Photometric data from the ASAS survey converted to the period  $P=176.027$  d. There are only a few points that indicate the shape of the primary and secondary minima.

## 6 CONCLUSIONS

We present our new project on study of long-period massive eclipsing binaries, where components are not synchronized and for this reason have not changed the evolution scenario of each other. The small sample of eleven binary systems was described here that was formed for the pilot spectroscopy with HRS/SALT. The software package FBS was developed by us for the analysis of spectral data. We describe this package and demonstrate its external accuracy in determination of stellar parameters. As the first result, we present the radial velocity curves and best-fit orbital el-

ements for both components of the FP Car binary system from our test sample.

**Acknowledgements** All spectral observations reported in this paper were obtained with the Southern African Large Telescope (SALT) under programs 2016-1-MLT-002, 2017-1-MLT-001 and 2019-1-SCI-004 (PI: Alexei Kniazev). AK acknowledges support from the National Research Foundation of South Africa. OM acknowledges support by the Russian Foundation for Basic Researches (Grant No. 20-52-53009). IK acknowledges support by the Russian Science Foundation (Grant No. 17-72-20119). LB acknowledges support by the Russian Science Foundation (Grant Nos. 18-02-00890 and 19-02-00611).

## References

- Andersen, J. 1991, *A&A Rev.*, 3, 91
- Avvakumova, E. A., & Malkov, O. Y. 2014, *MNRAS*, 444, 1982
- Avvakumova, E. A., Malkov, O. Y., & Kniazev, A. Y. 2013, *Astronomische Nachrichten*, 334, 860
- Bailey, J. D., & Landstreet, J. D. 2013, *A&A*, 551, A30
- Barnes, S. I., Cottrell, P. L., Albrow, M. D., et al. 2008, in *Proceedings of the SPIE 7014*, 70140K
- Bramall, D. G., Sharples, R., Tyas, L., et al. 2010, in *Proceedings of the SPIE 7735*, 77354F
- Bramall, D. G., Schmoll, J., Tyas, L. M. G., et al. 2012, in *Proceedings of the SPIE 8446*, 84460A
- Brancewicz, H. K., & Dworak, T. Z. 1980, *Acta Astronomica*, 30, 501
- Brown, T. M., Baliber, N., Bianco, F. B., et al. 2013, *PASP*, 125, 1031
- Buckley, D. A. H., Swart, G. P., & Meiring, J. G. 2006, in *Proceedings of the SPIE 6267*, 62670Z
- Cannon, A. J. 1926, *Harvard College Observatory Bulletin*, 837, 1
- Coelho, P. R. T. 2014, *MNRAS*, 440, 1027
- Crause, L. A., Sharples, R. M., Bramall, D. G., et al. 2014, in *Proceedings of the SPIE 9147*, 91476T
- Crawford, S. M., Still, M., Schellart, P., et al. 2010, in *Proceedings of the SPIE 7737*, 773725
- Delfosse, X., Forveille, T., Ségransan, D., et al. 2000, *A&A*, 364, 217
- Docobo, J. A., Tamazian, V. S., Malkov, O. Y., Campo, P. P., & Chulkov, D. A. 2016, *MNRAS*, 459, 1580
- Dvorak, S. W. 2004, *Information Bulletin on Variable Stars*, 5542, 1
- Fernandes, J., Lebreton, Y., Baglin, A., & Morel, P. 1998, *A&A*, 338, 455
- Gorda, S. Y., & Svechnikov, M. A. 1998, *Astronomy Reports*, 42, 793
- Gray, D. F. 1992, *The Observation and Analysis of Stellar Photospheres*, 20
- Hempel, M., & Holweger, H. 2003, *A&A*, 408, 1065
- Henry, T. J. 2004, in *ASPC*, 318, *Spectroscopically and Spatially Resolving the Components of the Close Binary Stars*, eds. R. W. Hilditch, H. Hensberge, & K. Pavlovski, 159
- Henry, T. J., Franz, O. G., Wasserman, L. H., et al. 1999, *ApJ*, 512, 864
- Houk, N., & Cowley, A. P. 1975, *University of Michigan Catalogue of Two-dimensional Spectral Types for the HD Stars. Volume I. Declinations -90. to -53*
- Husser, T. O., Wende-von Berg, S., Dreizler, S., et al. 2013, *A&A*, 553, A6
- Kaufer, A., Stahl, O., Wolf, B., et al. 1996, *A&A*, 305, 887
- Khaliullin, K. F., & Khaliullina, A. I. 2007, *MNRAS*, 382, 356
- Khaliullin, K. F., & Khaliullina, A. I. 2010, *MNRAS*, 401, 257
- Kniazev, A. Y., Gvaramadze, V. V., & Berdnikov, L. N. 2016, *MNRAS*, 459, 3068
- Kniazev, A. Y., Usenko, I. A., Kovtyukh, V. V., & Berdnikov, L. N. 2019, *Astrophysical Bulletin*, 74, 208
- Kovaleva, D. A. 2001, *Astronomy Reports*, 45, 972
- Lanz, T., & Hubeny, I. 2003, *ApJS*, 146, 417
- Lanz, T., & Hubeny, I. 2007, *ApJS*, 169, 83
- Malkov, O. Y. 2003, *A&A*, 402, 1055
- Malkov, O. Y. 2007, *MNRAS*, 382, 1073
- Malkov, O. Y., Oblak, E., Avvakumova, E. A., & Torra, J. 2007, *A&A*, 465, 549
- Malkov, O. Y., Piskunov, A. E., & Shpil’Kina, D. A. 1997, *A&A*, 320, 79
- Malkov, O. Y., Tamazian, V. S., Docobo, J. A., & Chulkov, D. A. 2012, *A&A*, 546, A69
- Newville, M., Stensitzki, T., Allen, D. B., et al. 2016, *Lmfit: Non-Linear Least-Square Minimization and Curve-Fitting for Python*, ascl:1606.014
- Nieva, M. F., & Przybilla, N. 2012, *A&A*, 539, A143
- O’Donoghue, D., Buckley, D. A. H., Balona, L. A., et al. 2006, *MNRAS*, 372, 151
- Pojmanski, G. 1997, *Acta Astronomica*, 47, 467
- Popper, D. M. 1980, *ARA&A*, 18, 115
- Tassoul, J.-L. 1987, *ApJ*, 322, 856
- Tassoul, J.-L. 1988, *ApJL*, 324, L71
- Torres, G., Andersen, J., & Giménez, A. 2010, *A&A Rev.*, 18, 67
- Zahn, J. P. 1975, *A&A*, 41, 329
- Zahn, J. P. 1977, *A&A*, 500, 121